Census of Active Super Massive Black Holes at z=1-2

Masayuki Akiyama (Astronomical Institute, Tohoku Univ.)

In order to investigate the accretion activities of SMBHs in the era of violent growth, we construct black hole mass and Eddigton ratio distribution functions (BHMF and ERDF) of X-ray-selected broad-line AGNs at z=1.1-1.7 in the Subaru XMM-Newton Deep Survey field. To properly account for selection effects, we derive the corrected BHMF and ERDF by applying the Maximum Likelihood method, assuming that the ERDF is constant regardless of the black hole mass. If we compare the corrected BHMF with that in the local Universe, the corrected BHMF at z=1.4 has a higher number density above 10^8 Msolar but a lower number density below that mass range. The evolution can be indicative of a down-sizing trend of accretion activity among the SMBH population. The evolution of ERDF from z=1.4 to 0 indicates that the fraction of AGNs with accretion rate close to the Eddington-limit is higher at higher redshifts. (K.Nobuta, M.Akiyama, et al. 2012, ApJ, 761, 143)

A sample of z~1.4 AGNs is constructed from X-ray observations of the SXDS field with XMM-Newton (Ueda et al. 2008 , see Figure 1). In this study, only X-ray sources in the region covered with deep optical imaging data taken with Suprime-Cam on the Subaru telescope (Furusawa et al. 2008) are considered. There are 733 and 576 AGN candidates in the soft-band and hard-band selected samples. Considering sources common to both samples, there are 896 unique AGN candidates. In order to identify the X-ray sources spectroscopically, optical and NIR spectroscopic observations are conducted. The spectroscopic observations identify 586 out of the 896 sources. The remaining 310 sources cannot be identified spectroscopically, mostly because of their faintness. For such objects, photometric redshifts have been estimated using the HyperZ photometric redshift code with galaxy and QSO SED templates. From the photometric redshift determination, not only their photometric redshifts, but also their types of SED can be constrained. In Figure 2, the absorption-corrected 2-10keV luminosity of AGNs are shown as a function of redshift. The absorption-corrected 2-10keV luminosity of AGNs distribute between log L2-10keV= 43-45 (erg/s) in the redshift range of z=1-2. The SXDS AGNs cover the most important part of the accretion growth of the SMBHs: AGNs in the luminosity range dominate the hard X-ray luminosity density of the Universe in the redshift range and the hard X-ray luminosity density as a function of redshift peaks at z=1 (Aird et al. 2010)

Figure 1

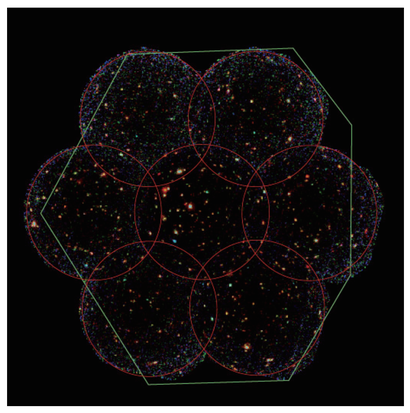

Figure 2

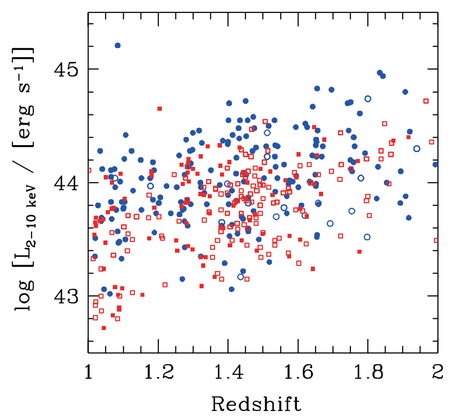

7 Assuming that the scaling relationship between luminosity and broad-line region size derived by reverberation mapping for local AGNs is applicable to AGNs at high-redshifts, black hole masses of broad-line AGNs can be estimated from their continuum luminosities and line widths of the broad-lines. We estimate the black hole mass of z~.4 AGNs with MgII broad-line widths measured in the optical spectra. An example of the measurement of the FWHM of broad MgII line is shown in Figure 3. As the optical spectroscopy does not cover the entire sample, we supplement these with Halpha broad-line widths measured in the NIR spectra. Examples of the measurements of the FWHM of the broad Halpha line are shown in Figure 4. The measured line width of Halpha line is converted to that of MgII line using the relation between the FWHMs of broad MgII and Halpha line as shown in Figure 5. For most of the objects, we derive 3000A monochromatic luminosity using the best-fit power-law continuum. For mildly obscured broad-line AGNs, the 3000A luminosity can be affected by dust extinction. Additionally for low-luminosity AGNs, the 3000A luminosity can be affected by a host galaxy component. In such cases, we estimate the intrinsic 3000A luminosity from the observed 2-10keV luminosity using the relation shown in Figure 6. The distribution of broad-line AGNs in the measured MgII FWHM vs intrinsic 3000A monochromatic luminosity plane is shown in Figure 7. Large open squares indicate the FWHMs that are estimated with the broad Halpha line . The solid lines indicate the constant MBH line. The dashed line indicate the constant Eddington ration lines. In the right panel, the distribution of broad-line AGNs at redshifts between 1.18 and 1.68 are shown.

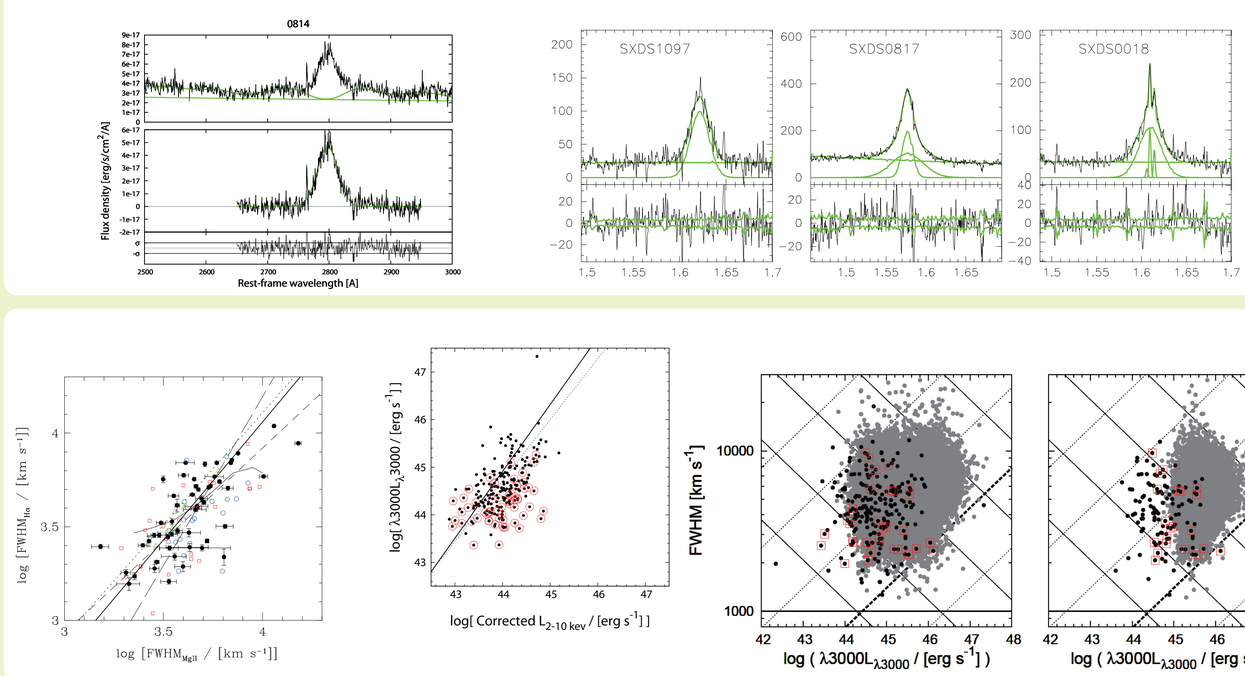

First we derive the binned BHMF and ERDF for the broad-line AGNs between 1.18<z<1.68 using the Vmax method. The resulting BHMF is shown in Figure 8 with filled circles for soft-band-selected broad-line AGNs. The binned BHMF have a peak at around MBH=10^8.5Msolar. The bineed ERDF is shown in Figure 9 and 10. In order to examine the MBH dependence of the binned ERDF, the binned ERDFs derived with the soft-band selected AGNs in the MBH range between 10^8.0-8.5 Msolar and that between 10^8.5-9.0 Msolar are plotted with blue filled cirfles and red filled diamonds, respectively. The overall shapes of the binned ERDFs do not significantly differ from each other within the uncertainty, except for the lowest Eddington ratio range where the lower mass binned ERDF can be affected by the flux limit.

Both of the BHMF and ERDF are affected by the detection limit determined by the X-ray count rate. In order to properly account for selection effects that impact the binned estimates, we derive the corrected BHMF and ERDF by applying the Maximum Likelihood method, assuming that the ERDF is constant regardless of the black hole mass. BHMF and ERDF are modeled with Schechter or double-power-law and Schechter or log-normal distributions, respectively. The resulting corrected BHMF and ERDF are shown in Figure 8 and 10. The corrected BHMF follows the estimated number density with the Vmax method well in the mass range above 10^8.5 Msoloar. The corrected ERDF is consistent with that derived in the 10^8-9 Msolar mass range with the Vmax method.

In Figure 8, the binned and corrected BHMFs are compared with the binned and estimated BHMF from the SDSS sample (Shen & Kelly 2012, blue circles and blue solid lines). The SXDS binned BHMFs is larger than the binned BHMF of the SDSS sample by two orders of magnitude at 10^8 Msolar. This is mostly because AGNs with lower Eddington ratio are detected in the SXDS sample than in the SDSS. The z~1.4 BHMFs are compared with the corrected BHMF in the local Universe (Schulze & Wisotzki 2010). The corrected BHMF at z~1.4 exceeds that of the local Universe in the mass range above 10^8 Msoloar. However the behaviour in the lower mass range is different; the local broad-line AGN BHMF shows a steep increase with decreasing black hole mass even below 10^7 Msolar, on the contrary, the SXDS sample shows a turn-over at a mass of 10^8.5 Msoloar.

As shown in Figure 9, both of the binned and corrected ERDF show a decline at Eddington ratio of 1. Such a distribution suggests that the accretion of X-ray-selected AGNs is limited by the Eddington luminosity. We compare the corrected ERDF with the estimated ERDF at z~1.4 from the SDSS sample. The shapes of the ERDFs match rather well. In the same figure, we also plot the corrected ERDF in the local Universe (Schulze & Wisotzki 2010). The shape of the corrected ERDF in the local Universe has a knee at a similar Eddington ratio, but shows a steeper increase in the low Eddington ratio range. The evolution of the corrected ERDF from z=1.4 to 0 indicates the fraction of AGNs with the Eddington ratio close to 1 is higher at higher redshifts.